Interaction of Ferricytochrome *c* with Zwitterionic Phospholipid Bilayers: A Raman Spectroscopic Study

James S. Vincent
Chemistry Department, University of Maryland Baltimore County, 5401 Wilkens Avenue, Catonsville, Maryland 21228
Ira W. Levin*
Laboratory of Chemical Physics, National Institute of Diabetes and Digestive and Kidney Diseases, National Institutes of Health, Bethesda, Maryland 20892

Received September 16, 1987; Revised Manuscript Received December 4, 1987

ABSTRACT: The vibrational Raman spectra of both pure L-α-dipalmitoylphosphatidylcholine (DPPC) liposomes and DPPC multilayers reconstituted with ferricytochrome *c* under varying conditions of pH and ionic strength are reported as a function of temperature. Total integrated band intensities and relative peak height intensity ratios, two spectral scattering parameters used to determine bilayer disorder, are invariant to changes in pH and ionic strength but exhibit a sensitivity to the bilayer concentration of the ferricytochrome *c*. Protein concentrations were estimated by comparing the 1636 cm^{-1} resonance Raman line of known ferricytochrome *c* solutions to intensity values for the reconstituted multilayer samples. Temperature-dependent profiles of the 3100–2800 cm^{-1} C–H stretching, 1150–1000 cm^{-1} C–C stretching, 1440 cm^{-1} CH_2 deformation, and 1295 cm^{-1} CH_2 twisting mode regions characteristic of acyl chain vibrations reflect bilayer perturbations due to the weak interactions of ferricytochrome *c*. The DPPC multilamellar gel to liquid-crystalline phase transition temperature, T_M, defined by either the C–H stretching mode I_{2935}/I_{2880} or the C–C stretching mode I_{1061}/I_{1090} peak height intensity ratios, is decreased by $\sim$4 °C for the $\sim 10^{-4}$ M ferricytochrome *c* reconstituted DPPC liposomes. Other spectral features, such as the increase in the 2935 cm^{-1} C–H stretching mode region and the enhancement of higher frequency CH_2 twisting modes, which arise in bilayers containing $\sim 10^{-4}$ M protein, are interpreted in terms of protein penetration into the hydrophobic region of the bilayer.

Physical studies designed to emphasize the thermotropic behavior of multilamellar model membranes reconstituted from a variety of saturated, symmetric acyl chain phospholipids serve to distinguish and to clarify the many interactions and reorganizations reflected by the bilayer matrix and its components [see, for example, Chapman (1982) and Killian and de Kruijff (1986)]. The major bilayer rearrangement of aqueous dispersions of these lipid systems is the endothermic gel to liquid-crystalline phase transition, whose characteristic temperature (T_M) is a function of lipid chain length, saturation, head-group composition, and bilayer perturbant. For pure multilayers composed of zwitterionic, saturated chain, diacylphosphatidylcholine lipids, for example, two additional, less energetic phase transitions have been observed at temperatures below the formation of the liquid-crystalline state. These transitions, the subtransition (Chen et al., 1980) and pretransition (Janiak et al., 1979), have been identified, respectively, as the introduction of hindered rotational motion of the acyl chains about the molecular axis during the conversion of the bilayer crystalline phase to the fully hydrated gel phase and, at higher temperatures, the formation of a ripple bilayer surface structure. The latter, intermediate ripple phase also exhibits faster molecular rotation, as measured on the NMR time scale (Westerman et al., 1982). The acyl chains of the lipid bilayer in the metastable gel phase, above the subtransition, exhibit several gauche conformers near the bilayer center. The chains acquire additional gauche conformers on increasing temperature as the bilayers enter the ripple phase and then ultimately undergo the first-order gel to liquid-crystalline phase transition. For hydrated, multilamellar L-α-dipalmitoylphosphatidylcholine (DPPC) bilayer dispersions, in particular, various physical techniques indicate that the gel to liquid-crystalline phase transition occurs at $\sim$41.5 °C, while the pretransition is induced at $\sim$35 °C. The subtransition occurs in the 15–18 °C temperature range depending upon the conditions reflecting sample history (Levin and Adams, unpublished observations; Chen et al., 1980).

The interaction of ferricytochrome *c* with various lipid systems has been studied by several spectroscopic techniques, including electron spin resonance (ESR) spin-labeling methods (Birrel & Griffith, 1976), resonance energy transfer (Tessie, 1981), fluorescence polarization (Faucon et al., 1976), and ^{13}C and ^{31}P nuclear magnetic resonance (NMR) spectroscopy (De Kruijff & Cullis, 1980; Brown & Wüthrich, 1977). These experimental approaches have established that cytochrome *c* does not bind to zwitterionic lipids represented, for example, by the dipalmitoylphosphatidylcholine (DPPC) bilayer system. In contrast, significant binding does occur with bilayers comprised of acidic lipids (Devaux & Seigneuret, 1985; Devaux et al., 1986). Although the weak interactions that may originate between zwitterionic lipids and cytochrome *c* are obviously extremely difficult to observe spectroscopically, their characterization could prove important for a more complete understanding of the role of cytochrome *c* in mitochondrial electron-transport processes (Daum, 1985; Gupte et al., 1984). An assessment of these subtle interactions and their subsequent effect on bilayer lipid conformational and dynamic properties is also necessary in order to clarify the effects of extrinsic bilayer proteins within the hydrophobic regions of the membrane. For example, McElhaney (1986) summarizes the experimental evidence for various peripheral membrane polypeptides and proteins in which both surface electrostatic interactions and intrinsic hydrophobic interactions, resulting from partial protein penetration, compete to varying extents in the formation of associated species. By specifically examining the cytochrome *c*/zwitterionic DPPC complex, we endeavor to emphasize the molecular details of the bilayer destabilization step in which protein segments penetrate the bilayer matrix

and interact directly with the lipid chains.

Vibrational Raman and infrared spectroscopy is a particularly sensitive technique for investigating changes in the structural and motional properties of lipids resulting from small intermolecular perturbations (Levin, 1984; Lord & Mendelsohn, 1981; Mantsch et al., 1986; Yeager & Gaber, 1987). These perturbations, which are manifest by changes in spectral band shapes, intensities, and frequency shifts, are conveniently monitored as a function of temperature. For example, the spectral details of the 3100–2800 cm^{-1} C–H stretching mode region correspond primarily to lipid interchain interactions (Gaber & Peticolas, 1977; Spiker & Levin, 1976; Mendelsohn et al., 1976), although a small amount of intrachain disorder is superimposed upon the lateral chain–chain effects (Huang et al., 1982). Alterations in the C–C stretching mode region (1150–1050 cm^{-1}) of the liposomal spectra reflect changes in the intramolecular trans/gauche conformation ratios within the acyl chains (Yellin & Levin, 1977). In addition, the acyl chain methylene deformation ($\sim$1440 cm^{-1}) and the methylene twisting ($\sim$1295 cm^{-1}) spectral regions are sensitive to lattice subcell packing configurations and other intermolecular reorganizations (Bush et al., 1980).

The Raman spectra of both pure DPPC liposomes and DPPC multilayers reconstituted with ferricytochrome *c* under various pH and ionic strength conditions are reported in this paper. The sensitivity of the vibrational spectra to weak ferricytochrome *c*—lipid interactions within the hydrophobic bilayer region is emphasized by presenting the data in the form of topological maps in which the horizontal axes represent the wavenumber and temperature variables and the vertical axis displays the Raman scattering intensity. Because of the highly linear and reproducible characteristics of the Raman spectrograph's intensified diode array detector, these contour maps provide extremely sensitive representations of the spectral changes resulting from small perturbations in the molecular system. Raman spectra of the pure and reconstituted multilamellar systems are compared as functions of temperature over a range including the subtransition, the pretransition, and the main gel to liquid-crystalline phase transition of the unperturbed bilayer form.

Materials and Methods

L-α-Dipalmitoylphosphatidylcholine (DPPC) was obtained from Avanti Polar Lipids and used without further purification. Ferricytochrome *c* (Sigma VI horse heart) was purified by chromatography through a CM-cellulose column according to the procedure of Brautigan et al. (1978). The integrity of the ferricytochrome *c* was verified by visible spectroscopy. The multilayer dispersions of DPPC were prepared by heating 10 mg of lipid mixed with 1 mL of water or buffer to 50 °C (above the gel to liquid-crystalline transition) for 10 min and mixing mechanically. Thorough mixing was assured by cycling the sample temperature through T_M and by constant agitation. The samples were sealed in glass capillary tubes, and the multilayers were compacted in a hematocrit centrifuge. Samples were stored in a refrigerator at 2–8 °C for at least 24 h before the spectra were recorded.

Ferricytochrome *c* bilayers were reconstituted in one of two ways: (a) polycrystalline DPPC was dispersed in a water or buffered aqueous solution containing ferricytochrome *c* and subsequently treated as in the pure liposomal DPPC case; (b) a pH-adjusted or buffered ferricytochrome *c* solution was added to an aqueous DPPC dispersion, heated to 50 °C, and agitated before the pH was readjusted. No differences were found in the spectral properties of liposomes from either preparation.

Raman spectra were normally observed as a function of temperature from 5 to 55 °C. The specific temperature range varied from experiment to experiment. A thermostated bath circulated heat-exchanged fluid through a thermoelectrically controlled sample holder, which also housed the thermocouple used for monitoring the bath temperature. A separate solid-state temperature-sensitive device controlled the power supplied to the thermoelectric temperature regulator. Spectra were normally obtained at 1 °C intervals from 5 to 55 °C. A Spectra Physics 165 Ar^+ laser provided the 514.5-nm exciting light. The intensity of the laser excitation ranged from 30 to 75 mW for the various experiments. The scattered light was collected with a Spex Triplemate spectrograph at a spectral resolution of $\sim$5–6 cm^{-1} and detected with an EG&G thermoelectrically cooled intensified silicon diode array. The operating conditions of the diode detector array were adjusted for linearity of response (Antcliff et al., 1984). A 1200 line/mm grating was used to span the 3100–2800 cm^{-1} and the 1600–900 cm^{-1} spectral regions. The spectrophotometer and temperature bath were controlled by a National Institutes of Health LDACS (laboratory data acquisition computer system) laboratory computer. This system enables programming (1) to monitor the sample temperature, (2) to change the thermoelectrically controlled temperature according to a prescribed protocol, (3) to allow a variable equilibration period (4 min between temperature changes for these experiments), and (4) to record the spectrum and transfer it as a file to a laboratory DEC PDP 11/70 computer for data storage before starting the next temperature-stepping sequence.

Results and Discussion

3100–2800 cm^{-1} C–H Stretching Mode Region

Pure DPPC Multilayers. Although the vibrational spectral characteristics of lipid assemblies have been described in detail before [see, for example, Levin (1984)], we briefly review the salient features. The C–H stretching mode region, 3100–2800 cm^{-1}, in the gel phase (<41 °C) consists of several distinct features. A peak at 2850 cm^{-1}, which is assigned to the symmetrical stretching modes of the acyl chain CH_2 groups, and a peak at 2880 cm^{-1}, superimposed upon a broad Fermi resonance background, comprise the major components of this spectral interval. The 2880 cm^{-1} transition is attributed to the asymmetric mode of the CH_2 groups of the acyl chains. The broad background arises from the Fermi resonance interaction between the symmetric CH_2 stretching modes, where the methylene groups are treated as coupled oscillators, and a manifold of CH_2 deformation overtone modes. In addition, transitions at 2873 and 2935 cm^{-1} correspond to a Fermi resonance doublet involving the hydrocarbon chain terminal methyl groups. This resonance interaction couples the methyl symmetric stretching mode and the first overtone of the methyl asymmetric deformation mode. The 2935 cm^{-1} feature is also superimposed upon a background derived from the Fermi resonance components involving the methylene moieties. The chain-terminal CH_3 asymmetric stretching modes occur at $\sim$2960 cm^{-1} and are accidentally degenerate with the choline methyl symmetric stretching modes. These features are illustrated in the low-temperature spectra displayed in Figure 1A.

In general, the vibrational transitions in the 3100–2800 cm^{-1} spectral region change in frequency and in intensity as the phospholipid multilayers increase in temperature and ultimately undergo a phase transition. These spectral changes are greatest, by far, for DPPC at the gel to liquid-crystalline phase transition temperature, $\sim$41.5 °C, as illustrated in

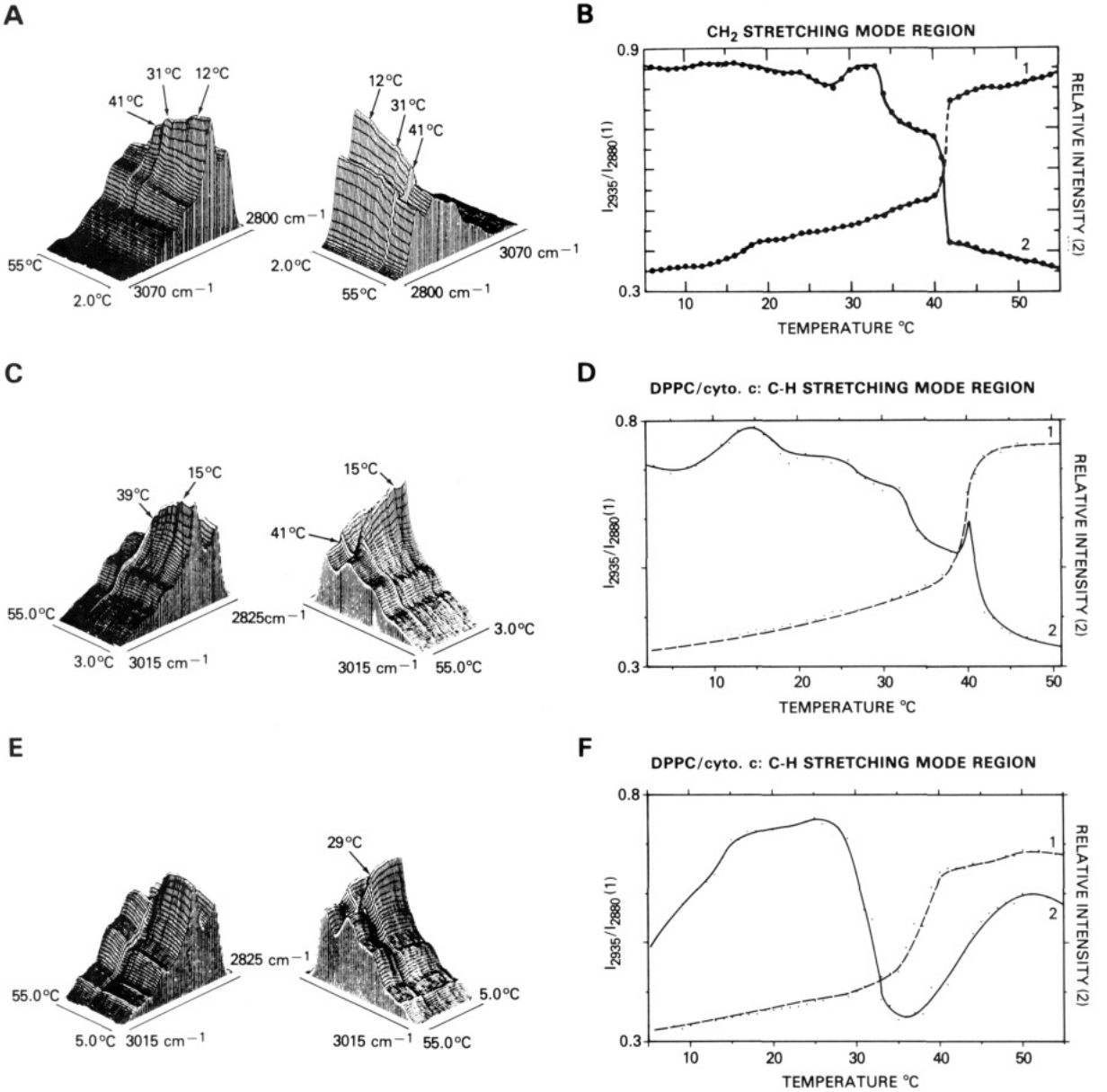

FIGURE 1: (A) Raman spectra of the 3070–2800 cm^{-1} C–H stretching mode region for pure DPPC dispersions in water over the 2.0–55.0 °C temperature span. (B) (Curve 1) I_{2935}/I_{2880} peak height intensity ratio of pure DPPC as a function of temperature. (Curve 2) Relative integrated intensity of the 3070–2800 cm^{-1} C–H stretching mode region of pure DPPC as a function of temperature. The scale at the left is for the peak height ratio curve (1). (C) Raman spectra of the 3015–2825 cm^{-1} C–H stretching mode region for DPPC dispersions in water mixed with ferricytochrome *c* (<10^{-5} M) at pH 7 over the 3.0–55.0 °C temperature span. T_M is 39.7 °C. (D) (Curve 1) I_{2935}/I_{2880} peak height intensity ratio plotted as a function of temperature for spectra in (C). (Scale at left.) (Curve 2) Relative integrated intensity of the 3015–2825 cm^{-1} C–H stretching mode region for the sample in (C) plotted as a function of temperature. (Scale at right.) (E) Raman spectra of the 3015–2825 cm^{-1} C–H stretching mode region for DPPC dispersions in water mixed with ferricytochrome *c* (~10^{-4} M) at pH 7 over the 5.0–55.0 °C temperature span. T_M is 37.3 °C. (F) (Curve 1) I_{2935}/I_{2880} peak intensity ratio plotted as a function of temperature for spectra in (E). (Scale at left.) (Curve 2) Relative integrated intensity of the 3015–2825 cm^{-1} C–H stretching mode region for the sample in (E) plotted as a function of temperature. (Scale at right.)

Figure 1A. The 2880 cm^{-1} line decreases in intensity and shifts 6–8 cm^{-1} higher in frequency as the lipid proceeds through the gel to liquid-crystalline phase transition. The 2850 cm^{-1} line also decreases slightly in intensity and shifts 4–6 cm^{-1} higher in frequency upon the gel to liquid-crystalline transition. The feature around 2935 cm^{-1} has increased noticeably in intensity after the change in phase. These changes in the Raman scattering are quite obvious in Figure 1A in which the features around 2880 and 2935 cm^{-1} gradually decrease and increase, respectively, in intensity as the temperature increases until the abrupt change at T_M. The band shapes remain relatively unaltered as the temperature is increased above T_M. However, below T_M, there are several features in the Figure 1A contours which can be correlated with changes in the molecular motion and packing characteristics of the phospholipid bilayer. Around 16–18 °C, the subtransition temperature region, a slight intensity increase in the 2940–2900 cm^{-1} interval is coupled to a small decrease in the 2880 cm^{-1} peak. The entire spectral region from 2800 to ~3000 cm^{-1} increases in intensity as the temperature approaches 31 °C, indicating an increase in packing order prior to the onset of disorder that is associated with the pretransition at ~36 °C.

As a measure of primarily interchain order with some superposition of intrachain effects, the ratio of the peak height intensity around 2935 cm^{-1} to the intensity of the 2880 cm^{-1} peak (I_{2935}/I_{2880}) has proved useful (Levin, 1984). This ratio increases with increasing disorder and is illustrated in Figure 1B(1) for this series of spectra. The inflection, associated with

the subtransition at approximately 18 °C, is consistent with the increase in disorder which arises when the acyl chains begin to rotate independently in the lattice. As shown in Figure 1A, at approximately 36 °C the overall scattering intensity increases slightly in the 2940–2850 cm^{-1} interval prior to the pretransition, which occurs over the 34–35 °C temperature range. Figure 1B(2) displays the plot of the intensity integrated over the entire 3100–2800 cm^{-1} region as a function of temperature. The pretransitiion is readily detected by this parameter as noted by the decrease in overall scattering intensity for this temperature region (Levin, 1985). Since, to a first approximation, the observed integrated intensity is a function of the number of molecular scatterers within the volume sampled by the laser beam, the experimental intensity decrease is consistent with a lattice expansion occurring simultaneously with the ripple phase behavior. The dramatic main gel to liquid-crystalline phase transition is clearly observed in the contours displayed in Figure 1A and in the two order/disorder peak height ratio and integrated intensity parameters illustrated in Figure 1B(1) and Figure 1B(2). That is, there is an abrupt change in intensity in the 2935 and 2880 cm^{-1} intervals at T_M = 41.5 °C. The peak height I_{2935}/I_{2880} intensity ratio, plotted in Figure 1B(1), demonstrates the highly cooperative nature of the phase transition over the transition temperature region, where the width of the main phase transition ΔT_M is ~1.4 °C. The integrated scattering intensity curve, Figure 1B(2), mirrors the decrease in order at T_M, while the contours in Figure 1A illustrate the increase in intensity in the 2935 cm^{-1} region and the shift and decrease in intensity of the 2880 cm^{-1} feature in the transition interval. This intensity decrease results from changes in the underlying manifold of vibrational transitions as the coupling between oscillators breaks down during the chain-melting process.

Reconstituted Ferricytochrome c/DPPC Multilayers. The weak interactions of cytochrome *c* with zwitterionic DPPC multilayers induce line-shape modifications as the system undergoes the subtransition, pretransition, and the main phase transition processes. Experimental temperature profiles were obtained from samples of DPPC reconstituted with ferricytochrome *c* at two pH values, 4.0 and 7.0, with and without 0.5 M (or greater) NaCl, and with and without 0.1 M phosphate buffer. No apparent changes in the behavior of the temperature profiles could be ascribed to the changes in the pH, buffer, or salt concentration of the liposomal dispersions. Both Raman scattering parameters, the total integrated band intensity and the relative peak height intensity values which describe the various phase transitions, depend primarily upon the concentration of the ferricytochrome *c* within the volume of multilayers circumscribed by the excitation laser beam. The protein, however, does not distribute uniformly in the multilamellar dispersions. Since the intensity of color in the sample tube after centrifugation decreases gradually from a light red to the nearly white color of pure DPPC, it is impossible to place the sample tube in the laser beam at a point where the ferricytochrome *c* concentration will be constant from sample to sample. We illustrate this variation in the temperature profiles for two samples of the same preparation of DPPC multilayers dispersed with ferricytochrome *c* in a pH 7.0, 0.1 M phosphate buffer in Figure 1C,E. These two sets of profiles have distinctly different topologies, with a main phase transition temperature that varies from 39.7 °C (Figure 1C) to 37.3 °C (Figure 1E). The main phase transition temperatures (T_M) were determined from the temperature dependence of the characteristic peak height intensity ratios for the C–H (vide infra) and C–C stretching mode regions. Samples with a T_M lower than 41.5 °C have proportionately larger microscopic concentrations of ferricytochrome *c* perturbing the bilayer acyl chain region within the small volume of liposome sampled by the incident laser beam.

We estimate the concentration of ferricytochrome *c* in the DPPC dispersions from the intense resonance Raman spectral line at 1636 cm^{-1} exhibited by the protein. This ferricytochrome *c* resonance Raman signal is observed with the same grating position used to record the CH_2 deformation (1450 cm^{-1}), the CH_2 twisting (1295 cm^{-1}), and the C–C stretching (1100 cm^{-1}) modes. By comparing the intensity of the 1636 cm^{-1} resonance Raman line in lipid dispersions with frozen solution samples of ferricytochrome *c* of known concentration, we were able to estimate the concentration in the liposomal sample to well within an order of magnitude. Frozen samples were used to increase the signal to noise levels of the recorded spectra. Since scattering from ice differs from solution scattering, an additional estimate of the ferricytochrome *c* concentration was made by comparing the 1636 cm^{-1} resonance Raman line intensities of lipid/protein dispersions with those of known ferricytochrome *c* concentrations in reconstituted DPPC liposomes. These dispersions were thoroughly mixed but not pelleted by centrifugation, a process which alters the uniform protein distribution. Considerable signal averaging of the mixed aqueous dispersions was necessary to improve the signal to noise characteristics for these determinations. Comparisons of the resonance Raman intensity and the lipid Raman intensity in these latter samples permits placing the ferricytochrome *c* concentrations of the pelleted samples into two broad categories: (1) less than 10^{-5} M and (2) approximately 10^{-4} M. T_M's determined by the temperature dependence of the C–C stretching mode peak height intensity ratios, I_{1090}/I_{1130} or I_{1090}/I_{1061}, correlate with the estimated ferricytochrome *c* concentration. That is, the T_M of the protein/lipid complex decreases the greater the ferricytochrome *c* concentration. Although there is no definite stoichiometric binding of the ferricytochrome *c* to the DPPC multilayers, the extrinsic protein perturbations are sufficient to alter dramatically the Raman spectra reflecting acyl chain dynamics. Examples from experiments on these mixtures will illustrate the spectral changes due to the ferricytochrome *c* interactions with DPPC as the multilayer system proceeds through the subtransition, pretransition, and main transition stages.

Low laser power levels (30–75 mW) were used in order to eliminate any possible local heating effects on the lipid matrix due to β-band absorption of ferricytochrome *c* and subsequent transfer of energy to the lipid bilayer. To ensure that this type of heating did not arise, the lipid Raman spectra (C–H stretching mode region at 3100–2800 cm^{-1}) of a concentrated ferrocytochrome *c* sample (8/1 lipid to protein mole ratio) were examined as a function of incident laser power. The reduced protein has a larger absorbance at the laser excitation wavelength of 514.5 nm than the oxidized species. The sample was kept at 34.5 °C, a temperature just below the T_M of the test sample, where the intensity of the 2880 cm^{-1} band changes dramatically upon the gel to liquid-crystalline phase change. The peak intensity ratio I_{2850}/I_{2880} remained constant at 0.95 for laser power levels in the range 25–300 mW at the sample. The ratio increased to 0.99 at 400 mW. Moreover, the frequency of the 2880 cm^{-1} band maximum remained constant at power levels below 300 mW, shifting to higher frequencies above 400 mW. The low laser power levels between 30 and 75 mW, used in these experiments, were clearly not involved in the dramatic thermotropic behavior observed in the Raman

Table I: Phase Transition Parameters Derived from Raman Spectral Data for DPPC Dispersions and Ferricytochrome *c*/DPPC Recombinants

vibrational interval	bilayer dispersion	T_M[a] (°C) peak[f] ratios	T_M[a] (°C) integrated[g] intensity	ΔT_M[b] (°C)	ΔR_M[c]	T_P[d] (°C) peak[f] ratios	T_P[d] (°C) integrated[g] intensity	T_S[e] (°C) peak[f] ratios	T_S[e] (°C) integrated[g] intensity
C–H stretch, 3100–2800 cm^{-1}	pure lipid	41.4	41.5	1.4	0.26	34–35	34	18	–
	$<10^{-5}$ M cyt *c*	39.7	40	2.6	0.25	–	33	–	–
	$\sim10^{-4}$ M cyt *c*	37.3	–[i]	5	0.21	–	31	–	–
C–C stretch, 1150–1000 cm^{-1}	pure lipid	41.0	41	2.0	–	35–37	34–36	17	15–19
	$<10^{-5}$ M cyt *c*	39.6	39.5	2	–	–	33	–	–
	$\sim10^{-4}$ M cyt *c*	38.0	37–39	3	–	–	31	–	–
CH_2 deformation, $\sim$1440 cm^{-1} region	pure lipid	–	41	2	–	–	34	–	17
	$<10^{-5}$ M cyt *c*	–	40	2	–	–	33	–	–
	$\sim10^{-4}$ M cyt *c*	–	38	4	–	–	30–33	–	–
CH_2 twist, $\sim$1295 cm^{-1} region	pure lipid	–	41.5	2	–	–	34	–	–
	$<10^{-5}$ M cyt *c*	–	41.5	2	–	–	34	–	–
	$\sim10^{-4}$ M cyt *c*	38.6[h]	–	6	–	–	–	–	–

[a] T_M, main phase transition temperature. [b] ΔT_M, width of main phase transition. [c] ΔR_M, difference in the C–H stretching mode I_{2935}/I_{2880} peak height intensity ratio before and after the main phase transition. [d] T_P, pretransition temperature. [e] T_S, subtransition temperature. [f] Peak height intensity ratios I_{2935}/I_{2880} and I_{1090}/I_{1061} were used for the C–H and C–C stretching mode regions, respectively (see text). [g] Transition temperatures estimated from temperature-dependent plots of the integrated intensity for the designated spectral interval (see text). [h] Peak height intensity ratio I_{1303}/I_{1297} (see text). [i] Indicates either not applicable or not observed.

spectra of the ferricytochrome *c*/DPPC reconstituted lipid bilayers.

The Raman spectra of the C–H stretching mode region for two samples of varying concentration are illustrated in Figure 1C,E. The sample with the lowest ferricytochrome *c* concentration ($<10^{-5}$ M, T_M 39.7 °C) has a Raman temperature profile (Figure 1C) which shows a steadily decreasing 2880 cm^{-1} feature that abruptly accelerates its decline at 39 °C. At the same temperature, the spectral region from 3000 to 2900 cm^{-1} suddenly increases in intensity and, then at higher temperatures, decreases to a constant intensity. The peak height ratio (I_{2935}/I_{2880}) and the total integrated intensity of the band are derived from the Raman profiles and are shown in Figure 1D. The peak height ratio plot as a function of temperature [Figure 1D(1)] shows no evidenced for either a sub- or a pretransition but exhibits a slightly broadened (ΔT_M $\sim$2.6 °C) gel to liquid-crystalline main phase transition.

Table I summarizes the thermal data derived from the Raman spectral parameters for liposomes containing various concentrations of ferricytochrome *c*. The peak height intensity ratio profile, shown in Figure 1F(1), shows a distinct departure from that of the pure DPPC liposomes, as a consequence of the ferricytochrome *c* ($\sim10^{-4}$ M) perturbation to the bilayer. In particular, T_M is reduced to 37.3 °C for the greater protein concentration, and the transition breadth, indicating a significant decrease in cooperativity, is nearly 5 °C. The subtransition and pretransition observed in the pure lipid peak ratio profiles are not evident in these DPPC/ferricytochrome *c* complexes. Changes in the Raman profiles are mirrored in the integrated intensity plots for the various spectral regions. The beginning of the decrease in intensity around 30 °C in the 2880 and 2850 cm^{-1} features for the samples in Figure 1C,E indicates the start of the pretransition. This same pretransition indicator is seen in the integrated intensity curves of Figure 1D(2) and Figure 1F(2). In the sample with $<10^{-5}$ M ferricytochrome *c* concentration [Figure 1D(2)], the intensity curve displays a cusp with the maximum at the main phase transition temperature. This sudden increase in Raman intensity may be a manifestation of fluctuations both in sample density and in molecular interactions occurring particularly at the midpoint of the phase transition. This phenomenon has also been observed in pure systems in which the temperature interval was sampled every 0.1 °C (Green, Lewis, and Levin, unpublished observations).

The integrated Raman spectral intensity in the 3000 cm^{-1} region of the sample with the $\sim10^{-4}$ M ferricytochrome *c* concentration [Figure 1E and Figure 1F(2)] decreases at the start of the pretransition and continues with increasing temperature, reaching a minimum near the beginning of the main transition. The intensity then increases and reaches a steady value above the T_M of 37.3 °C. This intensity behavior differs from that of the other samples and provides another indication of the complex and perhaps variable nature of the interaction of ferricytochrome *c* with a lipid membrane.

The mode of interaction of ferricytochrome *c* with the zwitterionic bilayer probably first involves electrostatic interactions between the charged groups on the surface of the protein with the lipid head-group dipoles, thus laterally spreading the bilayer lipids. Since the protein/lipid recombinants were prepared by cycling through the main phase transition, the amino acid side chains of the protein probably penetrate the loosened lipid lattice. In comparison to pure DPPC bilayers, the 2935 cm^{-1} region of the protein/lipid complexes increases significantly in intensity. This specific intensity alteration has not been generally observed in the context of liposomal recombinants. We interpret this intensity increase as the effect of a more polar environment near the methyl termini at the bilayer center. It has been demonstrated that a change in environment can dramatically affect the methyl Fermi resonance interaction reflected by the intensity of the methyl symmetric stretching component at 2935 cm^{-1} (Hill & Levin, 1979). The polarity change within the bilayer may arise from the effects of protein penetration as well as an increased accessibility of water near the bilayer center.

The difference in the peak height intensity ratio, I_{2935}/I_{2880}, between the gel and the liquid-crystalline states, ΔR_M, has been used to estimate the entropy and, therefore, the enthalpy of melting of multilamellar lipid bilayers (Huang et al., 1982). The ΔR_M values of the DPPC mixtures of ferricytochrome *c* (Table I) show only a slight decrease from that of pure DPPC dispersions for the most dilute ($<10^{-5}$ M) sample; that is, the entropic and enthalpic changes are nearly the same as those for pure multilamellar systems. The most concentrated sample ($\sim10^{-4}$ M), however, has a reduced enthalpy of melting of approximately 7.3 kcal/mol, a decrease from that of 8.6 kcal/mol for pure DPPC dispersions, as calculated according to Huang et al. (1982) from Raman spectral parameters.

1150–1000 cm^{-1} C–C Stretching Mode Region

Pure DPPC Multilayers. The 1150–1020 cm^{-1} skeletal C–C stretching mode region, shown in Figure 2, provides spectral parameters for directly observing intramolecular trans–gauche

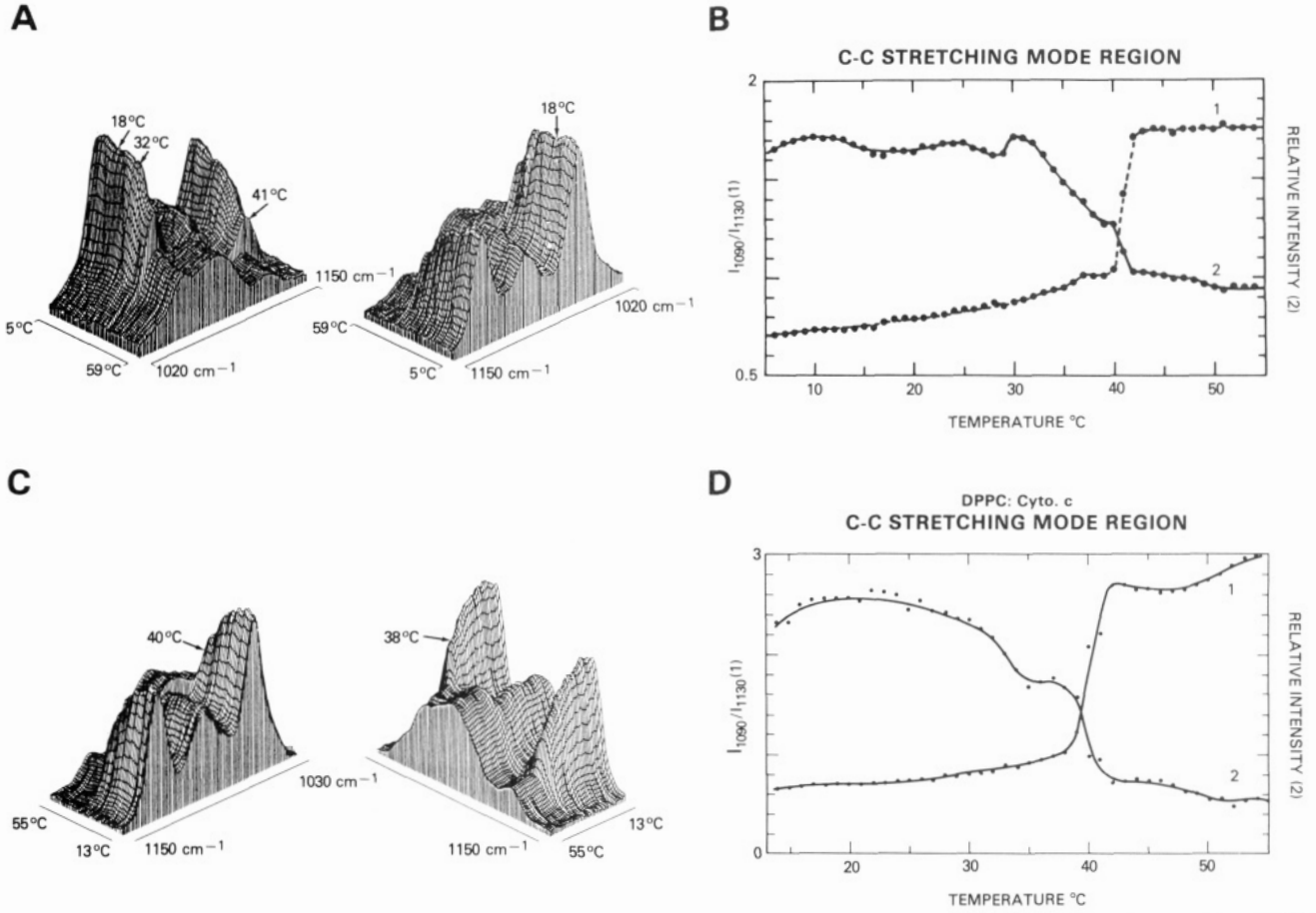

FIGURE 2: (A) Raman spectra of the 1150–1020 cm^{-1} skeletal C–C stretching mode region for pure DPPC dispersions in water over the 5.0–59.0 °C temperature span. (B) (Curve 1) I_{1090}/I_{1127} peak height intensity ratio plotted as a function of temperature for spectra in (A). (Scale at left.) (Curve 2) Relative integrated intensity of the 1150–1020 cm^{-1} skeletal C–C stretching mode region for the sample in (A) plotted as a function of temperature. (Scale at right.) (C) Raman spectra of the 1150–1030 cm^{-1} skeletal C–C stretching mode region for DPPC mixed with ferricytochrome *c* (<10^{-5} M) in water dispersions at pH 4, 0.1 M phosphate buffer over the 13.0–55.0 °C temperature span. T_M is 39.6 °C. (D) (Curve 1) I_{1090}/I_{1127} peak height intensity ratio plotted as a function of temperature for spectra in (C). (Scale at left.) (Curve 2) Relative integrated intensity of the 1150–1030 cm^{-1} region Raman spectra of the sample in (C) plotted as a function of temperature. (Scale at right.)

conformational changes within the acyl chains. Three all-trans C–C stretching modes are assigned to the frequencies at approximately 1061, 1097, and 1127 cm^{-1}. The frequency of the intense out-of-phase C–C stretching mode at 1061 cm^{-1} is relatively insensitive to temperature and to changes in the length of the acyl chain. However, the intensity of the 1061 cm^{-1} line has a local minimum near the subtransition temperatures (15–20 °C) and increases slightly near 32 °C before the sharp decrease during the pretransition region (34–40 °C) (Figure 2A). An abrupt decrease in the intensity of all three trans conformer features occurs at the main phase transition at 41.5 °C. The 1127 cm^{-1} in-phase C–C stretching mode and the relatively weaker 1097 cm^{-1} line are both temperature and chain length dependent. As the temperature increases and more gauche conformers occur, the 1127 cm^{-1} band decreases in intensity, shifting slightly to lower frequency, particularly after the gel to liquid-crystalline state phase transition.

Similar changes in intensity occur for the 1127 cm^{-1} feature as occur in the 1061 cm^{-1} band at the subtransition (15–20 °C) and pretransition (32–38 °C) temperatures. The spectral feature at ~1090–1085 cm^{-1}, which grows on increasing temperature, is assigned to the C–C stretching modes of the gauche conformers. An abrupt transition in the band shape is observed during the main phase transition at 41.5 °C. A qualitative measure of the relative number of gauche to trans conformers can be determined from the peak height intensity ratio, I_{1090}/I_{1127} (I_{gauche}/I_{trans}). This ratio for the C–C skeletal stretching modes is shown in Figure 2B(1) along with the integrated Raman scattering profile [Figure 2B(2)] over the 5–55 °C temperature range. The integrated intensity [Figure 2B(2)] again shows a small minimum around 15–18 °C and a peak at 30 °C before the strong decrease in intensity during the pretransition and main transition regions. Very few changes arise in either the band shapes or the total intensity of the C–C skeletal region at temperatures greater than 42 °C, that is, following the main phase transition.

Reconstituted Ferricytochrome c/DPPC Multilayers. Figures 2C,D illustrates the contours and temperature profiles for the Raman spectra of two reconstituted protein/lipid multilayers in the C–C skeletal stretching mode region of the spectrum. Both samples were prepared at pH 4 but with differing initial DPPC/protein mole ratios. The concentrations of the ferricytochrome *c* in the volumes illuminated by the laser beam differ considerably in the two samples due to the nonuniform distribution of the protein. One sample, made in 0.08 M phosphate buffer with an initial 175/1 mole ratio of DPPC/protein, yielded a ferricytochrome *c* concentration of <10^{-5} M in the volume sampled by the laser beam; the other sample, made with an initial 280/1 DPPC/protein mole ratio and no buffer, gave a concentration of protein of ~10^{-4} M. The presence or absence of phosphate buffer has not been found to alter the thermotropic behavior of this system. The T_M of the first sample was 39.6 °C, and the resonance Raman lines of the ferricytochrome *c* were barely visible, whereas the

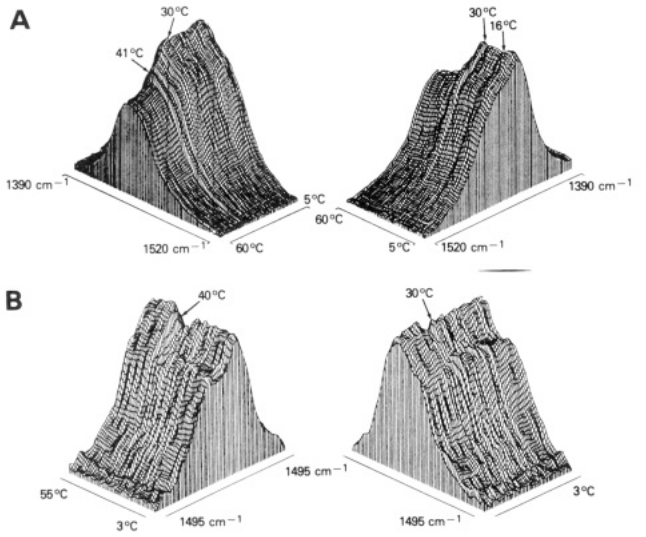

FIGURE 3: (A) Raman spectra of the 1520–1390 cm^{-1} CH_2 deformation mode region for pure DPPC/water dispersions over the 5.0–60.0 °C temperature span. (B) Raman spectra of the 1495–1395 cm^{-1} CH_2 deformation mode region of DPPC mixed with ferricytochrome *c* ($\sim 10^{-4}$ M) in water dispersions at pH 4, 0.1 M phosphate buffer over a temperature span of 3.0–55.0 °C.

resonance Raman bands of the second sample (T_M 38.0 °C) were quite prominent. The temperature contours of the Raman spectra of the C–C skeletal stretching modes for the $<10^{-5}$ M protein concentration sample are shown in Figure 2C, while the peak height intensity ratio and integrated intensity plots as a function of temperature appear in Figure 2D(1) and Figure 2D(2). The interaction of ferricytochrome *c* with DPPC is evident in the slightly reduced T_M and the disappearance of a distinct pretransition and subtransition in the peak height intensity ratio curve. Otherwise, the Raman spectra are quite similar to those of pure DPPC.

The Raman spectra of the DPPC liposomes containing high concentrations ($\sim 10^{-4}$ M) of ferricytochrome *c* exhibit prominent resonance Raman lines of ferricytochrome *c*. The increased concentration of ferricytochrome *c* considerably alters the temperature contours of the lipid spectra in the C–C stretching mode region. In particular, a ferricytochrome *c* resonance Raman band at ~ 1130 cm^{-1} complicates the profile derived from the I_{1090}/I_{1127} peak ratio plots. The ~ 1090 cm^{-1} marker, however, increases in intensity as the lipid mixture goes through the main phase transition, reflecting the increased number of gauche conformations in the liquid-crystalline state. Since the 1130 cm^{-1} feature, which is normally used to reflect the main phase transition, is not useful for constructing temperature profiles, the main phase transition temperatures cited in Table I were determined by using the I_{1090}/I_{1061} peak height intensity ratios. The band at 1061 cm^{-1} has no interfering protein resonance Raman band.

1440 cm^{-1} CH_2 Deformation Mode Region

Pure DPPC Multilayers. The Raman spectral region around 1437 cm^{-1}, attributed to the acyl chain CH_2 deformation modes, is shown in Figure 3A for the 5–60 °C temperature range. The overall line shapes undergo considerable change and, in general, decrease in intensity as the temperature increases. The slight decrease in the intensity around 16–18 °C probably corresponds to the subtransition. The intensity variations in this region are extremely sensitive to sample history (Adams and Levin, unpublished observations). Again, the scattering intensity increases at ~ 30 °C as the temperature approaches the pretransition. At the pretransition, the scattering intensity decreases, and a line shape change occurs (Figure 3A); the shoulder at 1455 cm^{-1} decreases in intensity and shifts to lower frequencies, finally merging into the 1440 cm^{-1} band at temperatures above the main phase transition.

Reconstituted Ferricytochrome c/DPPC Multilayers. The temperature profiles and integrated intensities of the 1437 cm^{-1} deformation mode for the $<10^{-5}$ M ferricytochrome *c* concentration sample are in general similar to those of pure DPPC (data not shown). In both the pure system and the dilute, protein-reconstituted multilayer, the peak at 1437 cm^{-1} shifts higher in frequency by about 4 cm^{-1}, the shoulder at approximately 1455 cm^{-1} disappears, and the overall intensity decreases as the lipid system undergoes the gel to liquid-crystalline phase transition. However, these changes are less pronounced for the reconstituted sample with $<10^{-5}$ M protein; that is, the pretransition and main transition are not as distinct, nor is the intensity decrease as great, for the lipid/protein mixture compared with the pure DPPC multilayers.

The temperature-dependent contours of the 1437 cm^{-1} CH_2 deformation mode of the more concentrated ($\sim 10^{-4}$ M) ferricytochrome *c*/DPPC dispersion also illustrate the significant interaction of the protein on the lipid bilayer (Figure 3B). The Raman intensity of this spectral region remains nearly constant throughout the 3–55 °C temperature range with the exception of the decline at the beginning of the pretransition near 30 °C, which reaches a minimum at 36 °C and rises to the initial value again at 40 °C. At higher temperatures, the 1437 cm^{-1} peak becomes more intense and broader while the shoulder at higher frequency remains virtually unchanged. This behavior is to be contrasted with the pure bilayer dispersion in which the intensities of the deformation region features decrease markedly in the liquid-crystalline form. Thus, the structural reorganizations required for the lipid to be transformed from the gel to the liquid-crystalline state in the presence of a relatively large ferricytochrome *c* concentration alter significantly the molecular polarizability changes modulated by the deformation modes during the phase transition. It is not clear at this time whether these effects are solely due to changes in acyl chain geometry or have an electronic origin due to the presence of the protein.

Table I summarizes the values of T_M for both the pure and protein-reconstituted multilayers. The T_M's were determined from the temperature dependence of the integrated intensity plots for the 1440 cm^{-1} region (data not shown).

1295 cm^{-1} CH_2 Twisting Mode Region

Pure DPPC Multilayers. Figure 4A illustrates the changes as a function of temperature in the spectral line shape of the CH_2 twisting modes around 1295 cm^{-1}. The intensity decreases gradually with increasing temperature, showing discontinuities at approximately 15–18 and 25–28 °C (Figure 4A). A distinct scattering decline begins at 32 °C, the start of the pretransition region. At 41.5 °C, the main phase transition temperature, the band shape changes abruptly. The peak shifts higher by about 6–8 cm^{-1}, and the band broadens. The changes in the integrated intensity at 41.5 °C is not as obvious as in the spectral representation (Figure 4A) because of the increased breadth of the band at temperatures above T_M. It is tempting to attribute this frequency shift and band broadening to the increased contribution of higher frequency twisting modes (Schachtschneider & Snyder, 1963). Since these modes include contributions of torsional components involving the terminal methyl group and the adjacent methylene group, as well as contiguous methylene units, to the CH_2 twisting normal coordinate, the overall increased chain disorder attendant upon the gel to liquid-crystalline phase transition permits these modes to be discerned.

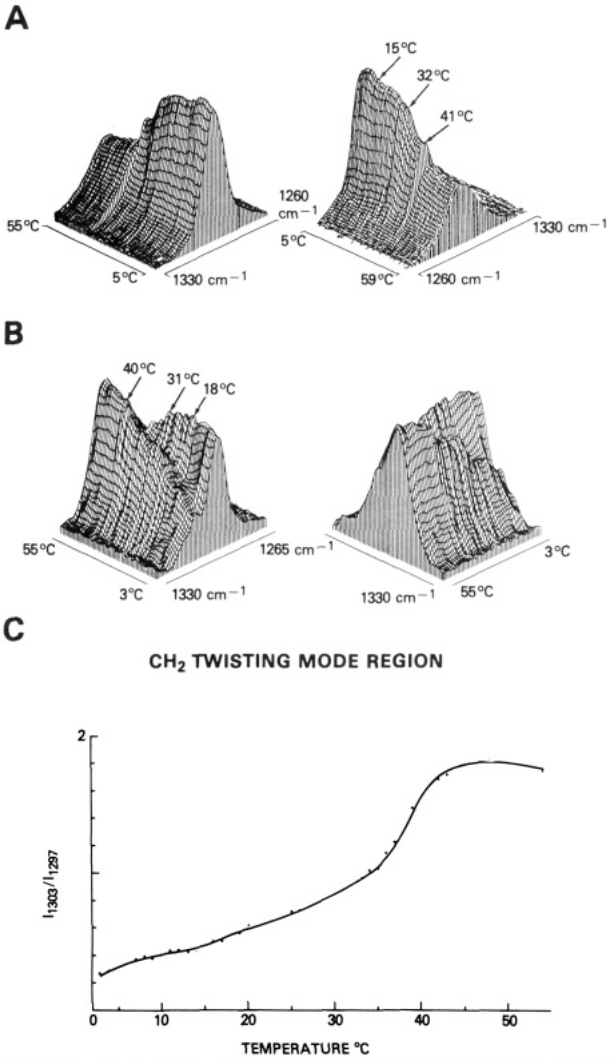

FIGURE 4: (A) Raman spectra of the 1330–1260 cm^{-1} CH_2 twisting mode region for pure DPPC/water dispersions over the 5.0–55.0 °C temperature span. (B) Raman spectra of the 1330–1265 cm^{-1} CH_2 twisting mode region of DPPC mixed with ferricytochrome *c* ($\sim 10^{-4}$ M) in water dispersions at pH 4, 0.1 M phosphate buffer over the 3.0–55.0 °C temperature span. (C) I_{1303}/I_{1295} peak height intensity plotted as a function of temperature for the spectra in (B).

Reconstituted Ferricytochrome c/DPPC Multilayers. The Raman spectra as a function of temperature of the 1295 cm^{-1} CH_2 twisting mode and the relative integrated intensity of this spectral region for the dilute $<10^{-5}$ M ferricytochrome *c* are also similar to those of pure DPPC (data not shown). However, the main transition in the protein complex begins at a lower temperature and appears broader than that of DPPC dispersions alone. The sharp peak at 1295 cm^{-1} of the gel state is replaced in the liquid-crystalline phase with a broader, slightly less intense band which has been shifted to 1300 cm^{-1}. The values of T_M determined from the temperature dependence of the integrated intensity in the 1300 cm^{-1} interval for both the pure multilayers and reconstituted protein systems are summarized in Table I.

Figure 4B illustrates the $\sim 10^{-4}$ M ferricytochrome *c*/DPPC sample CH_2 twisting mode, whose frequency at 1295 cm^{-1} for low temperatures shifts upward with increasing temperature to 1303 cm^{-1}. In contrast to the pure and dilute reconstituted liposomes, the 1303 cm^{-1} twisting modes are observed in the low-temperature phase. For these more concentrated ferricytochrome *c* concentrations, the protein apparently introduces the requisite low-temperature acyl chain disorder for enhancing the vibrational activity of the twisting modes normally observed in the disordered liquid-crystalline state. The peak intensity ratio of the 1303 and 1295 cm^{-1} features yields temperature-dependent plots (Figure 4C) similar to the temperature profile of a quantity passing through a phase transition. In this case, the observed "transition temperature" is 38.6 °C, a value close to the T_M of 38.0 °C derived from C–C stretching mode parameters.

CONCLUSIONS

As demonstrated by vibrational Raman spectral parameters, ferricytochrome *c*, a highly polar, basic protein, and DPPC, a zwitterionic lipid, form nonstoichiometric complexes capable of altering the bilayer-packing properties and the temperature-dependent behavior of the liposomal assemblies. Temperature profiles derived from the lipid acyl chain C–H stretching, C–C streching, CH_2 deformation, and CH_2 twisting mode regions were constructed from Raman spectral peak height intensity ratios and integrated band intensity measurements. Comparisons of these plots to those of pure DPPC liposomal dispersions indicate that the bilayer matrix experiences a variety of perturbations as a consequence of the weak protein interactions. The behavior of the temperature profiles derived from spectral parameters does not depend upon sample conditions of pH, buffer, or salt concentration but is correlated with the microscopic concentrations of ferricytochrome *c* in the portion of the lipid bilayer excited by the laser beam.

Ferricytochrome *c*, even at low concentration ($<10^{-5}$ M), significantly perturbs the structure of the lipid bilayer. Although the depression of T_M is small and the temperature profiles of the reconstituted liposomes closely resemble those of the pure DPPC multilayers, the addition of the protein suppresses both the pretransition and the subtransition behavior and increases the width of the main phase transition. The primary interaction at these protein concentrations appears to be electrostatic, although penetration of the protein into the bilayer hydrophobic acyl chain region, which may be small, leads to a significant membrane perturbation. A type II characterization, as defined by Papahadjopoulos et al. (1975) and discussed by McElhaney (1986), for ferricytochrome *c* at concentrations $>10^{-4}$ M is quite reasonable. In this case, T_M is significantly altered in comparison to the pure lipid multilayer, and the Raman spectral parameters indicate that the lipid acyl chains are spread due to the protein perturbation. This protein interaction with the lipid bilayers results in a partial penetration of the bilayer matrix by the protein side groups due to a combination of electrostatic and hydrophobic interactions. To a first approximation, the strictly dipolar interaction of either a zwitterionic or a charge-compensated ionic lipid with a protein, such as ferricytochrome *c*, with a large permanent dipole will be similar. However, a charged lipid can also interact specifically with oppositely charged protein side groups which displace the compensating ions and form stable protein/lipid ion pairs. This charged lipid/protein combination usually forms a relatively strong stoichiometric complex. Elucidation, however, of the subtle, but less specific, interactions of extrinsic proteins, such as ferricytochrome *c*, with zwitterionic lipid bilayers can perhaps provide important clues toward understanding the mechanisms of various membrane-mediated reactions.

Registry No. DPPC, 63-89-8; cytochrome *c*, 9007-43-6.

REFERENCES

Antcliff, R. R., Hillard, M. E., & Jarret, O., Jr. (1984) *Appl. Opt. 23*, 2369–2374.

Birrel, G. B., & Griffith, O. H. (1976) *Biochemistry 15*, 2925–2929.

Brautigan, D. L., Ferguson-Miller, S., & Margoliash, E. (1978) *Methods Enzymol. 53*, 128-148.
Brown, L. R., & Wüthrich, K. (1977) *Biochim. Biophys. Acta 468*, 389-395.
Bush, S. F., Adams, R. G., & Levin, I. W. (1980) *Biochemistry 19*, 4429-4436.
Chapman, D. (1982) *Biological Membranes* (Chapman, D., Ed.) Vol. 4, pp 179-229, Academic, New York.
Chen, S. C., Sturtevant, J. M., & Gaffney, B. J. (1980) *Proc. Natl. Acad. Sci. U.S.A. 77*, 5060-5063.
Daum, G. (1985) *Biochim. Biophys. Acta 822*, 1-42.
De Kruijff, B., & Cullis, P. R. (1980) *Biochim. Biophys. Acta 602*, 477-498.
Devaux, P. F., & Seigneuret, M. (1985) *Biochim. Biophys. Acta 822*, 63-125.
Devaux, P. F., Hoatson, G. L., Favre, E., Fellmann, P., Farren, B., MacKay, A. L., & Bloom, M. (1986) *Biochemistry 25*, 3804-3812.
Faucon, J. F., Dufourcq, J., Lussan, C., & Bernon, R. (1976) *Biochim. Biophys. Acta 435*, 283-294.
Gaber, B. P., & Peticolas, W. L. (1977) *Biochim. Biophys. Acta 465*, 260-274.
Gupte, S., Wu, E. S., Hoechli, L., Hoechli, M., Jacobson, K., Sowers, A. E., & Hackenbrock, C. R. (1984) *Proc. Natl. Acad. Sci. U.S.A. 81*, 2606-2610.
Hill, I. R., & Levin, I. W. (1979) *J. Chem. Phys. 70*, 842-851.
Huang, C., Lapides, J. R., & Levin, I. W. (1982) *J. Am. Chem. Soc. 104*, 5926-5930.
Janiak, M. J., Small, D. M., & Shipley, G. G. (1979) *J. Biol. Chem. 254*, 6068-6078.
Killian, J. A., & de Kruijff, B. (1986) *Chem. Phys. Lipids 40*, 259-284.
Levin, I. W. (1984) *Adv. Infrared Raman Spectrosc. 11*, 1-48.
Levin, I. W. (1985) *Chemical, Biological and Industrial Applications of Infrared Spectroscopy* (Durig, J. R., Ed.) pp 173-197, Wiley, New York.
Lord, R. C., & Mendelsohn, R. (1981) *Membrane Spectroscopy* (Grill, E., Ed.) pp 377-426, Springer-Verlag, New York.
Mantsch, H. H., Casal, H. L., & Jones, R. N. (1986) *Spectroscopy of Biological Systems* (Clark, R. J. H., & Hester, R. E., Eds.) pp 1-46, Wiley, New York.
McElhaney, R. N. (1986) *Biochim. Biophys. Acta 864*, 361-421.
Mendelsohn, R., Sunder, S., & Bernstein, H. J. (1976) *Biochim. Biophys. Acta 443*, 613-617.
Papahadjopoulos, D., Moscarello, M., Eylar, E. H., & Isac, T. (1975) *Biochim. Biophys. Acta 401*, 317-335.
Schachtschneider, J. H., & Snyder, R. G. (1963) *Spectrochim. Acta 19*, 117-168.
Spiker, R. C., & Levin, I. W. (1976) *Biochim. Biophys. Acta 455*, 560-575.
Tessie, J. (1981) *Biochemistry 20*, 1554-1560.
Westerman, P. W., Vaz, M. J., Strenk, L. M., & Doane, J. W. (1982) *Proc. Natl. Acad. Sci. U.S.A. 79*, 2890-2894.
Yeager, P., & Gaber, B. P. (1987) *Biological Applications of Raman Spectroscopy* (Spiro, T. G., Ed.) Vol. 1, pp 203-261, Wiley, New York.
Yellin, N., & Levin, I. W. (1977) *Biochemistry 16*, 642-647.

Lateral Interactions among Phosphatidylcholine and Phosphatidylethanolamine Head Groups in Phospholipid Monolayers and Bilayers†

Ken A. Dill* and Dirk Stigter
Departments of Pharmaceutical Chemistry and Pharmacy, University of California, San Francisco, California 94143
Received August 4, 1987; Revised Manuscript Received November 23, 1987

ABSTRACT: We develop theory for the lateral interactions among the zwitterionic head groups of phospholipids in monolayers and bilayers, particularly phosphatidylcholine (PC) and phosphatidylethanolamine (PE). With the P^- end of the head group anchored at the water/hydrocarbon interface, a balance of two effects dictates the angle that the P^-–N^+ dipole makes with respect to the plane of the bilayer: N^+ is driven toward water due to the (Born) electrostatic free energy, but the hydrophobic effect drives the methyl and methylene groups around the N^+ charge toward the hydrocarbon. The only adjustable parameter of the model is the average fluctuation of the oil/water interface or, alternatively, the dielectric constant of the hydrocarbon phase. The model predicts that at 5 °C the head group dipole should lie largely in the bilayer plane, in accord with X-ray, neutron diffraction, and NMR studies. The theory makes the novel prediction that the N^+ end of the dipole becomes increasingly submerged in hydrocarbon with increasing temperature, leading to strongly enhanced lateral repulsion between PC head groups. This prediction is in good agreement with second and third virial coefficients of monolayer lateral pressures, and with the temperature dependence of the former. The theoretical model is consistent with head group fluctuations measured by neutron diffraction of PC and PE bilayers. Because PE has a smaller hydrophobic cluster near N^+, its lateral repulsion should be much smaller and less temperature dependent than for PC, also in agreement with equation-of-state measurements. This suggests why at high density PE monolayers have higher melting temperatures than PC monolayers and more propensity for reversed curvature.

For some time there have been two paradoxical observations regarding interactions among the principal zwitterionic phospholipids. (i) Structural studies (X-ray diffraction, neutron diffraction, ^{31}P NMR) have shown similar packing of phosphatidylcholine (PC) and phosphatidylethanolamine (PE) head groups in bilayer membranes, yet their physical properties are very different: phase transition temperatures

† Supported by grants from the PEW Scholars Program and the NIH (to K.A.D.).

0006-2960/88/0427-3446$01.50/0